

# THE IMPLEMENTATION OF 3D UNDULATOR FIELDS IN THE UNAVERAGED FEL SIMULATION CODE Puffin

J. R. Henderson<sup>1</sup>, L.T. Campbell<sup>1,2,3,4</sup>, A.R. Maier<sup>3,4</sup> and B.W.J. McNeil<sup>1</sup>

<sup>1</sup>SUPA, Department of Physics, University of Strathclyde, Glasgow, UK

<sup>2</sup>ASTeC, STFC Daresbury Laboratory and Cockcroft Institute, Warrington, UK

<sup>3</sup>Center for Free-Electron Laser Science, Notkestrasse 85, Hamburg, Germany

<sup>4</sup>Institut für Experimentalphysik, Universität Hamburg, Hamburg, Germany

## Abstract

The FEL simulation code Puffin is modified to include 3D magnetic undulator fields. Puffin, having previously used a 1D undulator field, is modified to accommodate general 3D magnetic fields. Both plane and curved pole undulators have been implemented. The electron motion for both agrees with analytic predictions.

## INTRODUCTION

Puffin [1] is an unaveraged 3D FEL code which does not make the Slowly Varying Envelope Approximation (SVEA) or period averaging in its analytical model. As such, it is capable of modelling the a broad radiation field spectrum, full longitudinal broadband electron beam transport through the undulator, and Coherent Spontaneous Emission (CSE) emerging from current gradients in the beam.

However, although Puffin models a 6D electron beam and 3D radiation field, it does not employ a 3D magnetic undulator field. Instead, it implements a 1D undulator field with no off-axis variation. Superimposed, is an external focusing channel which is an approximation of the natural focusing found in a helical undulator. This focusing channel may be strengthened or weakened through the use of a ‘focusing factor’ [2] to obtain a desired betatron frequency.

Such a model does not simulate the detuning of the resonance condition in the transverse dimensions. Nor does it allow the focusing to emerge naturally from the off-axis variation of the magnetic fields. The resulting electron motion is an approximation in the case of a helical or curved-pole undulator; it is inaccurate in the case of an undulator with plane poles. Furthermore, the betatron motion as derived in Puffin is only valid when the electron beam is close to mono-energetic.

There is a need to model more realistic undulator fields; in particular, plane pole and curved pole undulators are more common than helical undulators for UV/X-ray FELs. There is therefore a requirement that various 3D planar undulator types be implemented in Puffin.

In the following, the Puffin model is first generalized to include general undulator magnetic fields. This model also allows a helical field description to be developed. Note also that this general magnetic field description need not be limited to undulators, and may allow future alternative applications of the Puffin code, to solve other radiation-electron interactions in static magnetic fields.

This general description is then used to implement both a generic plane pole and curved (canted) pole undulator FEL. Results are presented to demonstrate the correct electron motion and radiation characteristics are being solved.

## MODIFIED MATHEMATICAL MODEL

The derivation of the FEL system of equations modelled by Puffin is given in [1], using a magnetic undulator field  $\mathbf{B}_u = \frac{B_u}{2}(\mathbf{u}e^{ik_u z} + c.c.)$ , where  $\mathbf{u} = u_x \hat{\mathbf{x}} + iu_y \hat{\mathbf{y}}$  defines the polarization of the undulator. Following the same derivation, but using a general 3D magnetic field of the form  $\mathbf{B} = B_x \hat{\mathbf{x}} + B_y \hat{\mathbf{y}} + B_z \hat{\mathbf{z}}$ , one obtains the following system of equations:

$$\left[ \frac{1}{2} \left( \frac{\partial^2}{\partial \bar{x}^2} + \frac{\partial^2}{\partial \bar{y}^2} \right) - \frac{\partial^2}{\partial \bar{z} \partial \bar{z}_2} \right] A_{\perp} = - \frac{1}{\bar{n}_p} \frac{\partial}{\partial \bar{z}_2} \sum_{j=1}^N \bar{p}_{\perp j} L_j \delta^3(\bar{x}_j, \bar{y}_j, \bar{z}_{2j}) \quad (1)$$

$$\frac{d\bar{p}_{\perp j}}{d\bar{z}} = \frac{1}{2\rho} \left[ i b_{\perp} - \frac{\eta p_{2j}}{\alpha^2} A_{\perp} \right] - i \alpha \bar{p}_{\perp j} L_j b_z \quad (2)$$

$$\frac{dp_{2j}}{d\bar{z}} = \frac{\rho}{\eta} L_j^2 \left[ \eta p_{2j} (\bar{p}_{\perp j} A_{\perp}^* + c.c.) - i(1 + \eta p_{2j}) \alpha^2 (\bar{p}_{\perp j} b_{\perp j}^* - c.c.) \right] \quad (3)$$

$$\frac{d\bar{z}_{2j}}{d\bar{z}} = p_{2j} \quad (4)$$

$$\frac{d\bar{x}_j}{d\bar{z}} = \frac{2\rho\alpha}{\sqrt{\eta}} L_j \Re(\bar{p}_{\perp j}) \quad (5)$$

$$\frac{d\bar{y}_j}{d\bar{z}} = -\frac{2\rho\alpha}{\sqrt{\eta}} L_j \Im(\bar{p}_{\perp j}). \quad (6)$$

where

$$\eta = \frac{1 - \bar{\beta}_z}{\bar{\beta}_z} = \frac{\lambda_r}{\lambda_u}, \quad (7)$$

$$\begin{aligned} \bar{p}_{\perp} &= \frac{p_{\perp}}{mca_u}, & A_{\perp} &= \frac{eua_u l_g}{2\sqrt{2}\gamma_r^2 mc^2 \rho} E_{\perp}, \\ \rho &= \frac{1}{\gamma_r} \left( \frac{a_u \omega_p}{4ck_u} \right)^{2/3}, & a_u &= \frac{eB_0}{mck_u}, \\ \alpha &= \frac{a_u}{2\rho\gamma_r}, & b_{\perp} &= b_x - ib_y, \end{aligned} \quad (8)$$

and  $b_{x,y,z} = B_{x,y,z}/B_0$  are the scaled magnetic fields in  $x$ ,  $y$  and  $z$ , respectively, and  $B_0$  is the peak on-axis magnetic field. Other parameters remain as defined in [1]. The FEL parameter  $\rho$  above is defined using the peak undulator parameter, rather than the *r.m.s.* undulator parameter.

Using the above system of equations, one may use  $b_x$ ,  $b_y$  and  $b_z$  to define a static 3D magnetic field with which to simulate the energy exchange between a co-propagating electron beam and radiation field. The model is still subject to the same limitations as in [1], *i.e.* the paraxial approximation and the neglect of the backwards propagating wave.

Currently, two 3D undulator fields have been implemented in Puffin using this model, both derived from [3, 4]. The first is an undulator field with canted, or curved, pole faces, providing beam focusing in both transverse dimensions:

$$\begin{aligned} b_x &= \frac{\bar{k}_x}{\bar{k}_y} \sinh(\bar{k}_x \bar{x}) \sinh(\bar{k}_y \bar{y}) \sin(\bar{z}/2\rho), \\ b_y &= \cosh(\bar{k}_x \bar{x}) \cosh(\bar{k}_y \bar{y}) \sin(\bar{z}/2\rho), \\ b_z &= \frac{\sqrt{\eta}}{2\rho \bar{k}_x} \cosh(\bar{k}_x \bar{x}) \sinh(\bar{k}_y \bar{y}) \cos(\bar{z}/2\rho), \end{aligned} \quad (9)$$

where  $\bar{k}_{x,y}$  give the hyperbolic variation of the magnetic field in  $\bar{x}$ ,  $\bar{y}$ , and must satisfy

$$\bar{k}_x^2 + \bar{k}_y^2 = \frac{\eta}{4\rho^2}. \quad (10)$$

The second undulator type is a planar undulator with plane pole faces, described by:

$$\begin{aligned} b_x &= 0, \\ b_y &= \cosh(\sqrt{\eta} \bar{y}/2\rho) \sin(\bar{z}/2\rho), \\ b_z &= \sinh(\sqrt{\eta} \bar{y}/2\rho) \cos(\bar{z}/2\rho). \end{aligned} \quad (11)$$

## SIMULATIONS

The electron transport through both of these undulator types is well known. Some simple tests can therefore be designed to see if the electron motion in Puffin exhibits the correct behaviour.

As described in [3], a natural focusing channel arises from the off-axis variation of the magnetic field in the curved-pole undulator. From this so-called 'natural' focusing, one expects a slow oscillation characterised by betatron wavenumbers and corresponding matched beam radii in  $\bar{x}$  and  $\bar{y}$ , given, in the scaled notation, as:

$$\bar{k}_{\beta x} = \frac{a_u \bar{k}_x}{\sqrt{2\eta} \gamma_r}, \quad \bar{k}_{\beta y} = \frac{a_u \bar{k}_y}{\sqrt{2\eta} \gamma_r}, \quad (12)$$

$$\bar{\sigma}_x = \sqrt{\frac{\rho \bar{\epsilon}_x}{\bar{k}_{\beta x}}}, \quad \bar{\sigma}_y = \sqrt{\frac{\rho \bar{\epsilon}_y}{\bar{k}_{\beta y}}}. \quad (13)$$

respectively.

For the curved pole simulation,  $\rho = 0.0017$ ,  $a_u = 4.404$ ,  $\bar{\epsilon}_{x,y} = 1$  and  $\gamma_r = 575.63$ . A small electron pulse is used to generate a significant amount of coherent spontaneous

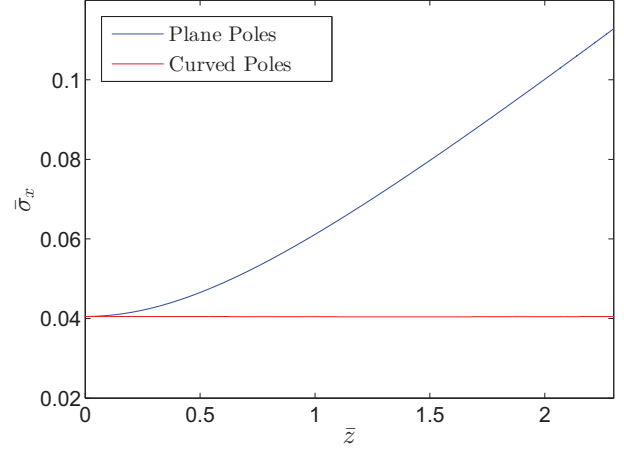


Figure 1: The electron pulse radius  $\bar{\sigma}_x$  plotted as a function of distance through the undulator.

emission (CSE) [5], to avoid a noisy transverse intensity distribution, allowing a simple check of the emitted radiation properties.

The radii in  $\bar{x}$  and  $\bar{y}$ , matched at injection, are seen to be constant throughout propagation.  $\bar{\sigma}_x$  is plotted against  $\bar{z}$  in Figure 1. In this case,  $\bar{k}_x = \bar{k}_y$ , which, from condition (10) and equation (12), results in

$$\bar{k}_{\beta x} = \bar{k}_{\beta y} = \frac{a_u}{4\rho \gamma_r}, \quad (14)$$

and, from (13), matched beam radii of  $\bar{\sigma}_{x,y} = 0.039$ , giving good agreement with Figure 1.

Similar to the curved-pole undulator, a natural focusing channel also arises in the plane-pole undulator, this time exclusively in the  $\bar{y}$  direction. For this simulation, the parameters used are identical to the curved pole case, except the beam energy and the undulator parameter are adjusted to  $\gamma_r = 238.04$  and  $a_u = 1.2876$ , to give the same betatron wavelength and transverse radii for comparison to the curved pole case.

The betatron period and matched beam radius in  $\bar{y}$  are now:

$$\bar{k}_{\beta y} = \frac{a_u}{2\sqrt{2}\rho \gamma_r}, \quad (15)$$

$$\bar{\sigma}_y = \sqrt{\frac{\rho \bar{\epsilon}_y}{\bar{k}_{\beta y}}}, \quad (16)$$

and electron motion in the  $(\bar{x}, \bar{p}_x)$  dimension should undergo free space dispersion when averaged over an undulator period, resulting in an expansion of the beam in the  $\bar{x}$  dimension.

The radius in  $\bar{x}$  during propagation is plotted in Figure 1, showing the beam expansion. The initial radius in  $\bar{x}$  is here set to the matched radius in  $\bar{y}$ , so  $\bar{\sigma}_x = \bar{\sigma}_y = 0.0327$ . The radius in  $\bar{y}$  remains constant, as expected.

Another test which can be made on the electron motion is that, again from [4],  $|\bar{p}_\perp|^2 = 0.5$  remains constant for all

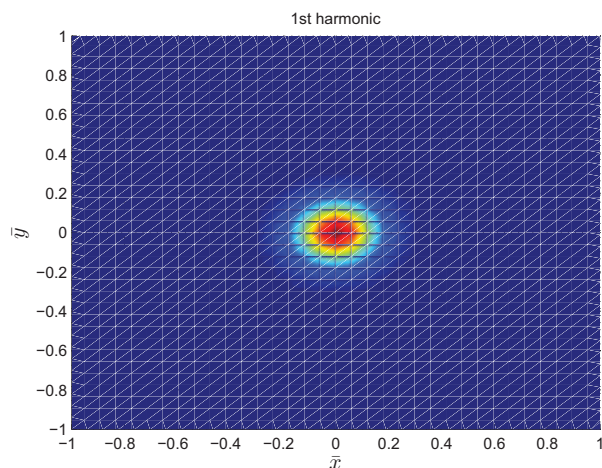


Figure 2: Transverse intensity profile of the 1<sup>st</sup> harmonic.

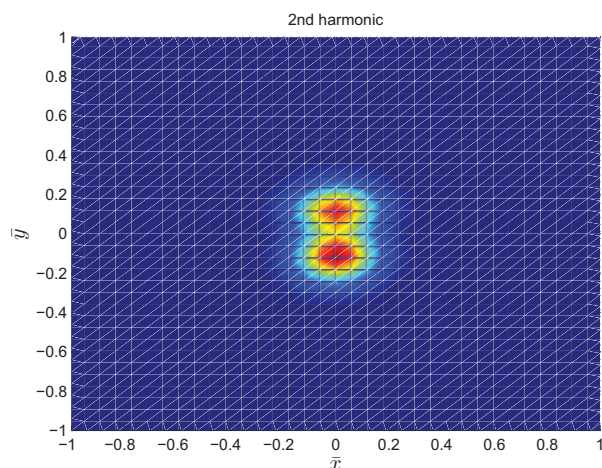


Figure 3: Transverse intensity profile of the 2<sup>nd</sup> harmonic.

electrons when averaged over an undulator period, which maintains a constant resonance condition throughout their betatron oscillations. This condition is seen to be satisfied in Puffin.

Puffin, being an unaveraged, non-SVEA code, is capable of the self-consistent simulation of the full radiation field spectrum in the FEL. The transverse intensity distributions of the first 2 harmonics in the plane-pole case from CSE is shown in Figures 2 and 3, showing the expected on-axis emission for the first harmonic and the off-axis emission for the second harmonic [6].

## CONCLUSION

The system of equations (1 - 6) have been derived in order to implement more realistic 3D undulators in Puffin, increasing the scope of the code.

The betatron oscillation of each electron arises naturally and self-consistently from the motion of the electrons in the specified undulator fields - it is not an approximation of the motion, which would only be valid for electrons close

to a given energy, super-imposed on top of another system of equations. Consequently, the functionality reported here will allow the simulation of broadband electron beams transported correctly through the FEL.

The work here may be combined with the model presented in [7], which describes how to employ a taper in the equations, to taper an undulator module's magnetic fields to and from zero over the first and last few undulator periods in each module. As well as more closely modelling a 'realistic' undulator, this avoids the task of calculating the correct initial conditions of the electron beam macroparticles that ensures a stable propagation along the undulator. This calculation can non-trivial, particularly for beams with a large energy spread.

Other static magnetic fields, such as quadrupoles, may be added to the equations. They would be subject to the same scalings presented here, which are specific to the FEL - for example,  $z$  is scaled to  $l_g$ , the FEL gain length. It is intended this will be done in the future.

## ACKNOWLEDGMENTS

We gratefully acknowledge the computing time granted by the John von Neumann Institute for Computing (NIC) and provided on the supercomputer JUROPA at Jülich Supercomputing Centre (JSC), under project HHH20; Science and Technology Facilities Council Agreement Number 4163192 Release #3; and ARCHIE-WeSt High Performance Computer, EPSRC grant no. EP/K000586/1

## REFERENCES

- [1] L.T. Campbell and B.W.J. McNeil, *Physics of Plasmas* **19**, 093119 (2012)
- [2] R. Bonifacio, L. De Salvo Souza, and B.W.J. McNeil, *Opt. Commun.* **93**, 179-185 (1992)
- [3] E.T. Scharlemann, *J. Appl. Phys.* **58**, 2154 (1985)
- [4] E.T. Scharlemann, in *High Gain, High Power FELs* (edited by R. Bonifacio et al ) (1989)
- [5] N. Piovela, *Phys. of Plasmas* **6**, 3358 (1999)
- [6] J.A. Clarke, *The Science and Technology of Undulators and Wigglers*, Oxford University Press (2004)
- [7] L.T. Campbell, B.W.J. McNeil and S. Reiche, *Investigation of a 2-Colour Undulator FEL Using Puffin*, MOPSO09, Proceedings of FEL 2013